DOI: 10.1534/genetics.104.029264

GLD-3 and Control of the Mitosis/Meiosis Decision in the Germline of *Caenorhabditis elegans*

Christian R. Eckmann,*[,1] Sarah L. Crittenden,* Nayoung Suh[†] and Judith Kimble*[,†,2]

**Howard Hughes Medical Institute and [†]Department of Biochemistry, University of Wisconsin, Madison, Wisconsin 53706*

Manuscript received March 26, 2004
Accepted for publication May 27, 2004

ABSTRACT

Germ cells can divide mitotically to replenish germline tissue or meiotically to produce gametes. In this article, we report that GLD-3, a *Caenorhabditis elegans* Bicaudal-C homolog, promotes the transition from mitosis to meiosis together with the GLD-2 poly(A) polymerase. GLD-3 binds GLD-2 via a small N-terminal region present in both GLD-3S and GLD-3L isoforms, and GLD-2 and GLD-3 can be co-immunoprecipitated from worm extracts. The FBF repressor binds specifically to elements in the *gld-3S* 3′-UTR, and FBF regulates *gld-3* expression. Furthermore, FBF acts largely upstream of *gld-3* in the mitosis/meiosis decision. By contrast, GLD-3 acts upstream of FBF in the sperm/oocyte decision, and GLD-3 protein can antagonize FBF binding to RNA regulatory elements. To address the relative importance of these two regulatory mechanisms in the mitosis/meiosis and sperm/oocyte decisions, we isolated a deletion mutant, *gld-3(q741)*, that removes the FBF-binding site from GLD-3L, but leaves the GLD-2-binding site intact. Animals homozygous for *gld-3(q741)* enter meiosis, but are feminized. Therefore, GLD-3 promotes meiosis primarily via its interaction with GLD-2, and it promotes spermatogenesis primarily via its interaction with FBF.

GERM cells can divide by either the mitotic or the meiotic cell cycle and, in animals, they can differentiate as either sperm or oocytes. These fundamental decisions are crucial for animal development and their misregulation can lead to clinical problems. For example, germline tumors are a frequent type of cancer (*e.g.*, Talerman 1985; Ulbright 2004), and defects in germline stem cells may underlie infertility (Fox and Reijo Pera 2001). However, the regulation of mitotic proliferation in the human germline remains poorly understood. Germline stem cells are regulated by signaling from a somatic niche in *Caenorhabditis elegans*, Drosophila, and probably vertebrates (Kimble and White 1981; Meng *et al.* 2000; Spradling *et al.* 2001). Within the germline, stem cells are maintained by RNA-binding proteins of the PUF [for *Pu*milio and *F*BF (***fem-3* b**inding **f**actor)] family in both *C. elegans* and Drosophila (Lin and Spradling 1997; Forbes and Lehmann 1998; Crittenden *et al.* 2002). In the human testis, Pumilio-2 is expressed in germline stem cells (Jaruzelska *et al.* 2003; Moore *et al.* 2003). Therefore, the molecular regulation of germline stem cells may be conserved throughout the animal kingdom.

We have focused on regulation of the mitosis/meiosis decision in *C. elegans*. Organization of the germline is essentially the same in the two sexes (XX self-fertilizing hermaphrodite and XO male; for review see Hubbard and Greenstein 2000). The mitotic region is located at the distal end; more proximally, germ cells transition into early meiotic prophase; and yet more proximally, germ cells enter the pachytene stage of meiotic prophase. Therefore, progression from mitosis into meiotic prophase is spatially organized in a linear fashion extending from the distal end. We note that virtually all germline "cells" are connected to a common core of cytoplasm, but we call them "cells" for several reasons: they do not divide synchronously, they adopt distinct fates within the syncytium (*e.g.*, mitosis *vs.* meiosis, sperm *vs.* oocyte), and each "cell" possesses its own cytoplasmic territory that is largely enclosed by a plasma membrane (reviewed in Hubbard and Greenstein 2000). Therefore, germline mitosis/meiosis and sperm/oocyte controls probably act at the level of individual "cells."

The mitotic region of the *C. elegans* germline includes germline stem cells (Crittenden *et al.* 2003). Unlike Drosophila, where a few well-defined stem cells are located adjacent to the niche (Xie and Spradling 2000; Yamashita *et al.* 2003), the *C. elegans* mitotic region comprises about 225 germ cells, most organized in a cylinder that extends ~20 cell diameters along the gonadal axis from the niche (Figure 2A; Table 2; Crittenden *et al.* 1994); specific stem cells within the mitotic region have not been identified. It seems most likely that *C. elegans* germline stem cells are not controlled by the lineage strategy typical of Drosophila germline stem cells, but instead by a regulative strategy, typical of many vertebrate stem cells (Watt and Hogan 2000). The regulative strategy generates distinct populations of

[1]*Present address:* Max Planck Institute of Molecular Cell Biology and Genetics, 01307 Dresden, Germany.

[2]*Corresponding author:* HHMI/Department of Biochemistry, 433 Babcock Dr., Madison, WI 53706-1544. E-mail: jekimble@facstaff.wisc.edu

TABLE 1

Summary of critical RNA regulators

Regulator	Molecular identity	Cell cycle		Sex determination	
		Mitosis	Meiosis	Oocyte	Sperm
FBF	PUF RNA repressor	+	−	+	−
GLD-1	STAR/GSG/*quaking* translational repressor	−	+	−	+
GLD-2	Atypical poly(A) polymerase	−	+	NA	NA
GLD-3	Bicaudal-C homolog	−	+	−	+
NOS-3	Nanos homolog	−	+	+	−

+, promotes fate; −, inhibits fate; NA, not applicable; see text for further explanation and references.

cells—some with stem cell potential and others that have begun to differentiate. In the *C. elegans* germline, a molecular understanding of how those populations are established is emerging (see DISCUSSION).

This article focuses on the role of GLD-3 (*germline development*) in controlling the mitosis/meiosis and sperm/oocyte decisions in the *C. elegans* germline. To place our GLD-3 studies in context, we first introduce other RNA regulators critical to these decisions. Table 1 summarizes their molecular identities and biological functions. Briefly, FBF-1 and FBF-2 are nearly identical and collectively are called FBF; they belong to the PUF family of RNA-binding proteins and control both mitosis/meiosis and sperm/oocyte decisions (ZHANG *et al.* 1997; CRITTENDEN *et al.* 2002). PUF proteins bind specifically to 3′-UTR regulatory elements and repress their target mRNAs (WICKENS *et al.* 2001). FBF controls germline fates, at least in part by repressing *gld-1* (CRITTENDEN *et al.* 2002). FBF achieves the switch from spermatogenesis to oogenesis together with NOS-3, one of three nematode Nanos homologs, by repressing *fem-3* (ZHANG *et al.* 1997; KRAEMER *et al.* 1999).

The decision to leave the mitotic cell cycle and enter meiosis is promoted by two GLD proteins (KADYK and KIMBLE 1998) and by NOS-3 (HANSEN *et al.* 2004). GLD-1 is a STAR/GSG/*quaking* RNA-binding protein and translational repressor (JONES and SCHEDL 1995; JAN *et al.* 1999). GLD-2 is the catalytic subunit of an atypical poly(A) polymerase (WANG *et al.* 2002). GLD-1 and GLD-2 act redundantly to promote the switch from the mitotic to the meiotic cell cycle (KADYK and KIMBLE 1998). Thus, in *gld-1* and *gld-2* single mutants, germ cells make the transition from mitosis into meiosis, but in *gld-1 gld-2* double mutants, the germline is largely mitotic with little or no entry into meiosis (KADYK and KIMBLE 1998). This synergistic effect suggested that *gld-1* and *gld-2* activities act in parallel to control entry into meiosis. The *nos-3* gene promotes GLD-1 accumulation and appears to act in the *gld-1* branch of regulation (HANSEN *et al.* 2004).

GLD-3 belongs to the Bicaudal-C family of RNA-binding proteins, and it has multiple roles in germline development (ECKMANN *et al.* 2002). In germline sex determination, GLD-3 controls continued spermatogenesis in males and the number of sperm produced in self-fertilizing hermaphrodites; in addition, GLD-3 is required for germline survival, progression through meiosis, and early embryogenesis (ECKMANN *et al.* 2002). GLD-3 interacts with GLD-2 as a subunit of an atypical poly(A) polymerase activity (WANG *et al.* 2002). Whereas the canonical poly(A) polymerase is monomeric and enriched in the nucleus (RAABE *et al.* 1994; MARTIN *et al.* 1999), the GLD-2/GLD-3 enzyme is heterodimeric and resides predominantly in the cytoplasm (ECKMANN *et al.* 2002; WANG *et al.* 2002).

In this article, we investigate the role of GLD-3 in the mitosis/meiosis decision. We show that GLD-3 works together with GLD-2 to control entry into meiosis and that it works in parallel to GLD-1 and NOS-3. In addition, we demonstrate that FBF acts upstream of GLD-3 in the mitosis/meiosis decision, binds the *gld-3S* 3′-UTR and represses GLD-3 protein expression. By contrast, GLD-3 acts upstream of FBF in the sperm/oocyte decision by antagonizing the binding of FBF to its 3′-UTR regulatory element (ECKMANN *et al.* 2002). To explore the relationships among FBF, GLD-3, and GLD-2, we first show that FBF and GLD-2 bind to distinct regions of GLD-3. We then generate a GLD-3 deletion mutant, *gld-3(q741)*, that removes the FBF-binding region, but leaves the GLD-2-binding region and KH domains intact. This *gld-3* deletion mutant is defective in the sperm/oocyte decision, but the mitosis/meiosis decision is virtually wild type. We conclude that GLD-3 promotes meiosis primarily via its interaction with GLD-2 and that it promotes spermatogenesis primarily via its interaction with FBF.

MATERIALS AND METHODS

Nematode strains and RNAi: Worm strains are derivatives of the wild-type Bristol strain N2 and were maintained at 20° as described by BRENNER (1974). All mutations used were either internal deletions or nonsense mutations, and all are putative nulls: LGI—*gld-1(q485)* (JONES and SCHEDL 1995), *gld-2(q497)* (KADYK and KIMBLE 1998; WANG *et al.* 2002); LGII—*fbf-1(ok91)*, *fbf-2(q704)* (CRITTENDEN *et al.* 2002), *gld-3(q730)* (ECKMANN *et al.* 2002). The *gld-3(q741)* allele was isolated in a PCR-based screen for deletion mutants induced by ethyl methane sulfonate [see KRAEMER *et al.* (1999) for

method], outcrossed against wild-type (Bristol, N2) eight times, and balanced with *mIn1*. Primers used for screening were as described (Eckmann *et al.* 2002). The deletion removes nt 1912–4076 in the genomic sequence, where the A in ATG is the first nucleotide. The *gld-3(q741)* mutation is recessive with respect to fertility and makes a few Fog hermaphrodites. To balance mutations linked to LGI, we used *unc-15(e73)* with a closely linked GFP transgene (*ccIs4251*), and to balance mutations on chromosome II, we used *mIn1[mIs14 dpy-10(e128)]*. Double, triple, and quadruple mutants on LGII were generated by recombination, balanced by *mIn1[mIs14 dpy-10(e128)]*, and validated by PCR for deletions or by sequencing for *q704*. Adult germline phenotypes were scored 24 hr past L4 stage at 20°.

***gld-3(RNAi)*:** By standard procedures (Kamath and Ahringer 2003), HT115 cells were transformed with a construct to generate double-stranded RNA corresponding to *gld-3* (nt 1–1719), a region common to both *gld-3S* and *gld-3L*. When animals were fed *gld-3(RNAi)* bacteria, defects were similar to those observed after injection of a similar *gld-3* region (Eckmann *et al.* 2002). Zygotic defects were visible in the first window (16–36 hr) after feeding. The success of *gld-3(RNAi)* for any given experiment was scored by continued feeding to ensure that later progeny displayed the maternal germline survival phenotype (Eckmann *et al.* 2002). In addition, *nos-3(q650) gld-3 (RNAi)* animals had the same phenotype as *nos-3(q650) gld-3(q730)* double mutants, and GLD-3 protein was either significantly decreased or undetectable when animals fed *gld-3(RNAi)* bacteria were immunostained for GLD-3 (data not shown).

DAPI staining and immunocytochemistry: Germlines were extruded from the animal and stained with 4,6-diamidino-2-phenylindole (DAPI) staining or immunocytochemistry by standard methods (Crittenden *et al.* 1994). The extent of each region was assayed by nuclear morphology using DAPI staining and confirmed using affinity-purified antibodies: anti-GLP-1 for the mitotic region (Crittenden *et al.* 1994), anti-HIM-3 (kindly provided by M. Zetka) for meiotic cells (Zetka *et al.* 1999), and anti-phosphohistone H3 (PH3) to mark cells in mitosis (Hendzel *et al.* 1997). Antibodies used for examining RNA regulators included: affinity-purified anti-GLD-1 (kindly provided by T. Schedl), anti-GLD-2 (Wang *et al.* 2002), anti-GLD-3 (Eckmann *et al.* 2002), anti-FBF-1 (Crittenden *et al.* 2002), and anti-NOS-3 (Kraemer *et al.* 1999). Anti-RME-2 antibodies (kindly provided by B. Grant) were used to demonstrate the production of oocytes in males. Positive controls for antibodies were included in all experiments. Epifluorescent images were captured with a Zeiss Axioskop equipped with a Hamamatsu digital CCD camera (Hamamatsu Photonics) and processed with Openlab 3.1.5 (Improvision).

Worm extracts, *in vitro* translation, immunoprecipitation, and yeast two hybrid: Worm extracts were generated by boiling worms in SDS sample buffer for 5 min. Protein separation was achieved on 4–12% gradient gels and subsequent immunoblots onto PVDF membranes were carried out according to standard procedures. Secondary antibodies were used as described (Eckmann *et al.* 2002).

In vitro translation in TNT-T7-coupled reticulocyte lysate was carried out according to the manufacturer's protocol (Promega). A full-length cDNA clone for *gld-3LΔ* was generated by RT-PCR from *gld-3(q741)* worms with primers including convenient restriction sites (*Eco*RI and *Sal*I). The open reading frame and the entire 3′-UTR was cloned into pTNT (Promega). A construct containing the entire *gld-3S* cDNA in pTNT was generated with similar primers.

For immunoprecipitation, N2 worms were grown on standard NGM agar plates, collected by centrifugation, and then washed multiple times in M9 buffer, with a final wash in NP40 extraction buffer (150 mm NaCl, 1.0% NP-40, 50 mm Tris, pH 8.0). The equivalent of 1 ml packed worms was resuspended in 5 ml total extraction buffer, supplemented with an EDTA-free protease inhibitor cocktail (Roche). Worms were frozen immediately in liquid nitrogen and homogenized with a cooled mortar and pestle. The frozen extract was thawed on ice, cleared by centrifugation at full speed for 20 min in a cooled Eppendorf tabletop centrifuge and diluted to 1 mg protein/1 ml buffer. For each immunoprecipitation, 500 μg extract was incubated with 10 μl preimmune serum or anti-GLD-2 antibody (Wang *et al.* 2002) coupled protein G beads (Pharmacia) for 2 hr at 4° on a rotating platform. Protein G beads were subsequently washed five times with 1 ml NP40 buffer. Bound proteins were eluted in SDS sample buffer, boiled, and separated on 4–12% gradient gels, which were then used to prepare Western blots. GLD-3L antibodies were used as a primary antibody as in Eckmann *et al.* (2002).

Yeast two-hybrid experiments were done as described by Eckmann *et al.* (2002). Full-length *gld-2* ORF in pACT is described in Wang *et al.* (2002). Fragments of *gld-3* ORF were inserted into pBTM116. Full-length *gld-3* ORF and N-terminal deletion is described in Eckmann *et al.* (2002).

Yeast three-hybrid and gel retardation assays: Three-hybrid experiments were performed as described by Bernstein *et al.* (2002). *gld-3S* RNA sequences were cloned into the *Xma*I and *Sph*I sites of the vector pIIIA/MS2-2, using either PCR-amplified fragments (an RNA segment containing FBE-a + b and RNA segment FBE-c) or annealed synthetic oligonucleotides (individual FBF-binding sites, FBE-a and FBF-b). For binding specificity, a mutation (UG to AC) was engineered by site-directed mutagenesis using Quickchange (Stratagene).

Fusion proteins were made as described by Crittenden *et al.* (2002). Purification of GST-FBF-1 protein was essentially carried out according to Crittenden *et al.* (2002) and dialyzed against 10 mm Hepes buffer, pH 7.9. *In vitro* binding reactions were performed with purified GST-FBF-1 protein incubated in the presence of buffer D (Ohno *et al.* 2000) supplemented with indicated radiolabeled and gel-purified *gld-3S* RNA fragments. The reactions were resolved on a 6% native polyacrylamide gel under standard conditions.

RESULTS

***gld-1* and *gld-3* activities are redundant for control of entry into meiosis:** To determine if *gld-3* acts in parallel to *gld-1*, we generated animals deficient for both *gld-1* and *gld-3* activities. We first found *gld-1; gld-3* double mutants to be inviable; characterization of that lethality is beyond the scope of this work. We therefore used RNAi to deplete *gld-3* activity in *gld-1* mutants (see materials and methods). The *gld-1; gld-3(RNAi)* germlines were tumorous: no nuclei typical of early meiosis were identified by DAPI staining (Figure 1A), the mitotic marker anti-PH3 stained many nuclei throughout the germline (Figure 1C), and the meiotic marker anti-HIM-3 was not detectable (Figure 1D). GLP-1, a marker that correlates with mitosis, was also evenly distributed throughout the *gld-1; gld-3(RNAi)* tumorous germlines (data not shown). The germlines of *gld-1 gld-2; gld-3(RNAi)* animals were also exclusively tumorous (Figure 1, E and F). Enlarged defective nuclei were frequent in *gld-1; gld-3 (RNAi)* germlines (60%, $n = 25$; Figure 1B), whereas these unusual nuclei were rare in *gld-1 gld-2* tumors (6%,

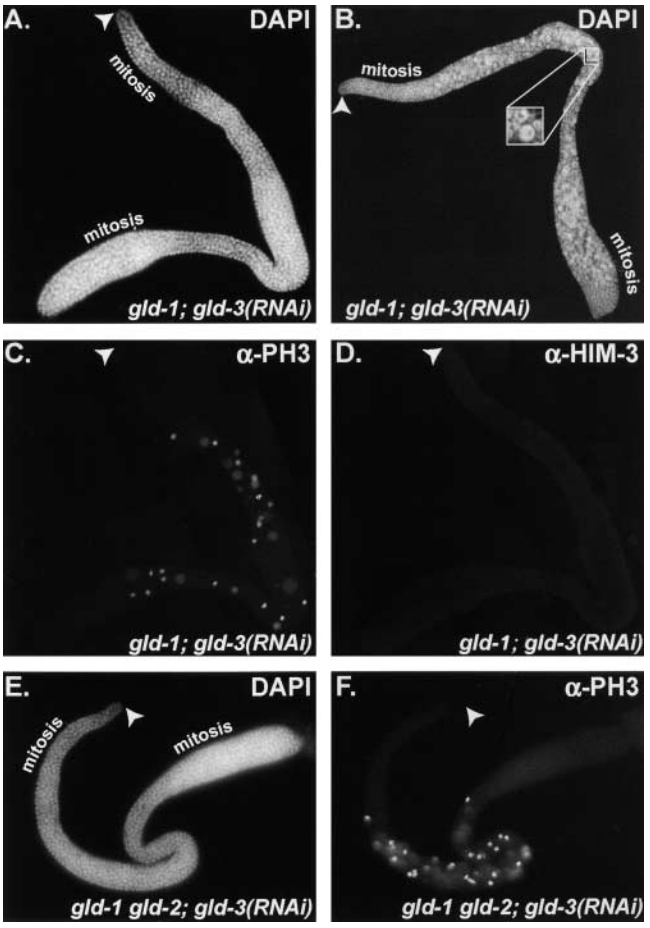

FIGURE 1.—*gld-1; gld-3* germlines are tumorous. Extruded germlines are from adult hermaphrodites. A, B, and E are stained with DAPI, C and F are stained with anti-phosphohistone 3, and D is stained with anti-HIM-3. Arrowhead, distal end of germline. (A–D) *gld-1; gld-3(RNAi)* germline is tumorous. (B) Enlarged nuclei in *gld-1; gld-3(RNAi)* germlines. Inset shows enlarged nuclei at increased magnification. (E and F) *gld-1 gld-2; gld-3(RNAi)* germline is tumorous. HIM-3 was absent from *gld-1 gld-2; gld-3(RNAi)* germlines (data not shown).

$n = 16$) and *gld-1 gld-2; gld-3(RNAi)* tumors (25%, $n = 18$). Therefore, *gld-1 gld-2* and *gld-1; gld-3* are similar, but not identical, germline tumors. We conclude that wild-type *gld-3* promotes meiosis in the absence of *gld-1*, and vice versa; therefore, these two genes appear to act in parallel to control entry into meiosis.

Entry into meiosis is delayed in *gld-2* and *gld-3* single mutants: Animals homozygous for either *gld-2* or *gld-3* possess a mitotic region (MR), transition zone (TZ), and pachytene region (PR) arranged normally (KADYK and KIMBLE 1998; ECKMANN *et al.* 2002). To ask if *gld-2* and *gld-3* single mutants have some minor defect in the transition from mitosis to meiosis, we examined the MR/TZ and TZ/PR borders. To measure the position of these borders, we counted number of nuclei along the distal-proximal axis from the distal end to the MR/TZ boundary and from the distal end to the TZ/PR boundary; in addition, we counted total number of nuclei in the MR; all measurements were made in DAPI-stained adult hermaphrodite germlines that had been extruded from the animals at 24 hr past L4. Some animals were also stained with the mitotic marker anti-phosphohistone (HENDZEL *et al.* 1997) and the meiotic marker anti-HIM-3 (ZETKA *et al.* 1999) to confirm the DAPI staining results (data not shown).

In wild-type animals, the MR extends ~20 nuclei along the distal-proximal axis and includes a total of ~225 nuclei (CRITTENDEN *et al.* 1994; Figure 2A; Table 2). By contrast, the MRs of *gld-2* and *gld-3* single mutants were longer and had more nuclei than normal (Figure 2, B and C; Table 2). The MR/TZ boundary was shifted to an average of ~27 or 28 nuclei in *gld-2* and *gld-3* mutant germlines (Table 2). Furthermore, the boundaries between MR and TZ and TZ and PR were not as sharp in *gld-2* and *gld-3* mutants as they were in wild-type germlines. In *gld-2* and *gld-3* single-mutant L4s, we observed a similar, although less pronounced, extension of the MR. By comparison, the MRs of *gld-1* and *nos-3* mutants were not longer than normal (Table 2). Indeed, the *gld-1* mitotic region was shorter (Table 2), suggesting that GLD-1 plays some minor role in maintaining mitosis in addition to its major role in directing entry into meiosis. We conclude that both *gld-2* and *gld-3* are required for determining the position at which germ cells enter meiosis and that removal of either activity extends the mitotic region.

We next examined animals lacking both *gld-2* and *gld-3*. If *gld-2* and *gld-3* act together to control entry into meiosis, then the double mutant should be no more defective than either single mutant. We first attempted to make a *gld-2; gld-3* double mutant, but it was inviable; therefore, these genes act synergistically in embryogenesis, but characterization of that synergy is beyond the scope of this work. We therefore depleted *gld-3* from *gld-2* mutants using RNAi. The transition from mitosis to meiosis in *gld-2; gld-3(RNAi)* germlines was virtually identical to that of *gld-2* and *gld-3* single mutants (Figure 2D; Table 2). Surprisingly, most *gld-2; gld-3(RNAi)* germ cells arrested in pachytene, a synthetic phenotype suggesting redundancy for progression into diplotene (data not shown). However, the focus of this article is entry into meiosis, and we emphasize the lack of a synergistic effect for *gld-2* and *gld-3* in the mitosis/meiosis decision.

GLD-2/GLD-3 molecular interaction: The genetic analyses described above indicate that GLD-2 and GLD-3 work together to control entry into meiosis. Consistent with this hypothesis, GLD-2 and GLD-3 function biochemically as subunits of an atypical poly(A) polymerase (WANG *et al.* 2002). The *gld-3* gene encodes two major proteins, GLD-3L and GLD-3S; in the N-terminal half, these two proteins share five KH motifs as well as parts of a serine-rich region (ECKMANN *et al.* 2002; Figure 3A). The larger protein, GLD-3L, possesses a C-terminal extension that binds FBF (ECKMANN *et al.* 2002). To learn what part of GLD-3 is responsible for its specific

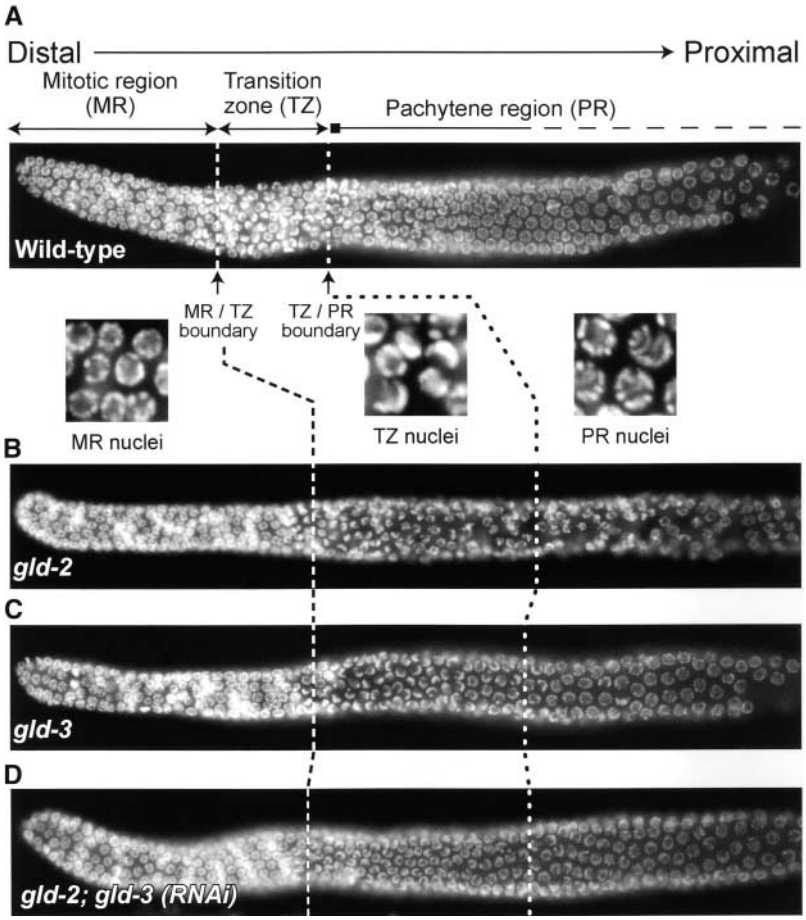

FIGURE 2.—*gld-2* and *gld-3* mutants have an extended mitotic region. Germlines were extruded, stained with DAPI, and scored for mitotic region (MR), transition zone (TZ), and pachytene region (PR). MR nuclei have either dispersed chromatin or condensed chromosomes typical of mitosis; TZ nuclei in early meiotic prophase I (leptotene/zygotene) display a crescent of condensed chromosomes (DERNBURG *et al.* 1998), and PR nuclei possess fully paired chromosomes. The mitotic region begins at the distal end and extends to the MR/TZ boundary, defined as the first circumferential ring of nuclei with ~80% crescent-shaped nuclei (dashed line); the transition zone extends to the TZ/PR boundary, which is defined as the first circumferential ring of nuclei with ~80% pachytene nuclei (dotted line). All germlines were dissected from adult hermaphrodites of the same approximate stage; magnification the same in each image. (A) Wild-type germline. (B) *gld-2 (q497)*, (C) *gld-3(q730)*, and (D) *gld-2(q497); gld-3 (RNAi)* germlines. Controls for the efficiency of *gld-3(RNAi)* are described in MATERIALS AND METHODS. The mitotic region extends farther proximally in these mutants than in wild type. See Table 2 for quantitation.

binding to GLD-2, we generated GLD-3 deletion mutants and assayed them for interactions with GLD-2 by yeast two-hybrid assay. Full-length GLD-3L interacts with GLD-2, as do two N-terminal GLD-3 fragments containing amino acids 1–81 or 34–81 (Figure 3B). These N-terminal fragments did not bind FBF (data not shown). An N-terminal fragment containing amino acids 55–81 failed to interact with GLD-2, suggesting that amino acids 34–55 are required for GLD-2 interaction. Furthermore, a large C-terminal fragment carrying

TABLE 2

Sizes of mitotic region and transition zones in *gld* single mutants

Genotype[a]	MR/TZ boundary (range)[b]	TZ/PR boundary (range)[b]	*n*	Total no. of gc in MR (range)[c]	*n*
Wild type	20 (18–21)	30 (28–31)	25	225 (190–278)	13
gld-1(q485)	14 (10–18)	23 (20–32)	15	175 (140–214)	6
gld-2(q497)	28 (25–34)	49 (43–54)	30	338 (292–387)	3
gld-3(q730)	27 (23–32)	41 (38–45)	8	276 (235–323)	3
gld-3(q741)	22 (19–26)	36 (33–40)	20	240 (215–290)	3
nos-3(q650)	18 (13–24)	28 (20–38)	16	255 (240–275)	4
gld-2; gld-3(RNAi)	29 (24–34)	52 (41–58)	18	339 (303–385)	5
gld-1; gld-3(RNAi)	Tumorous[d]	Tumorous[d]	60	Tumorous[d]	60
gld-1 gld-2; gld-3(RNAi)	Tumorous[d]	Tumorous[d]	32	Tumorous[d]	32

n, number of germlines scored; MR, mitotic region; TZ, transition zone; PR, pachytene region; gc, germ cells; see Figure 2 and text for explanation.

[a] All mutations, except *gld-3(q741)*, were strong loss-of-function putative nulls (see MATERIALS AND METHODS and RESULTS).

[b] Range indicates the shortest boundary and the longest boundary observed.

[c] As in footnote *b* except range indicates lowest and highest germ cell counts in data sets.

[d] All or virtually all germ cells are in mitosis.

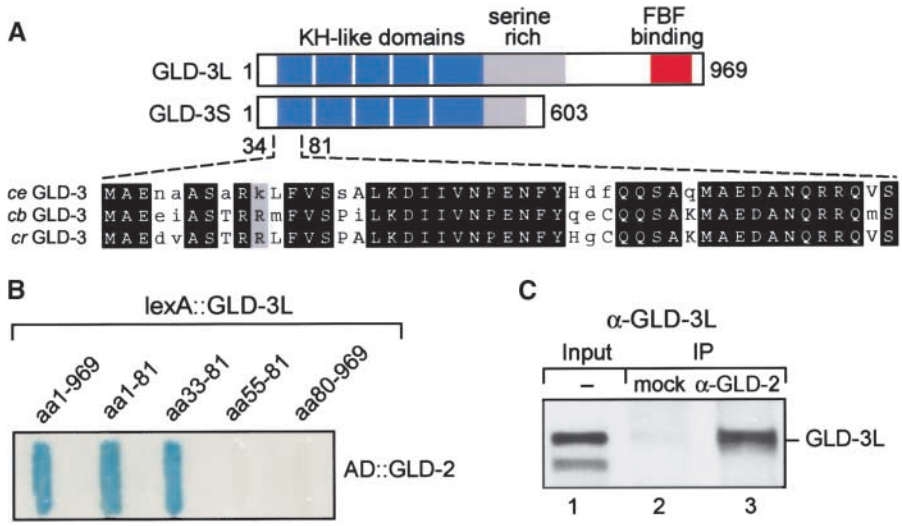

FIGURE 3.—GLD-3 N terminus binds to GLD-2. (A, Top) *gld-3* encodes two major proteins, GLD-3L and GLD-3S. Shared domains include five KH domains (blue) and a serine-rich region (gray). GLD-3L bears an FBF-binding region in its C-terminal extension (red). (Bottom) Minimal GLD-2-binding region with amino acid sequences provided for three Caenorhabditis species (*ce*, *C. elegans*; *cb*, *C. briggsae*; and *cr*, *C. remanei*). (B) Yeast two-hybrid assays for GLD-2/GLD-3 interaction, β-galactosidase activities. (C) Co-immunoprecipitation (ID) of GLD-3L using anti-GLD-2 (α-GLD-2) immune serum, but not with preimmune serum (mock). Note smaller breakdown product of GLD-3L visible in input lane.

amino acids 80–969 failed to interact with GLD-2 (Figure 3B), but did retain its ability to bind FBF (ECKMANN *et al.* 2002). In addition, an N-terminal fragment of GLD-3 (amino acids 1–102) binds GLD-2 *in vitro* (data not shown). Interestingly, aa 34–81 are strongly conserved in GLD-3 homologs from each of three Caenorhabditis species (Figure 3A). We conclude that specific binding to GLD-2 is conferred by a small region that is present in both GLD-3L and GLD-3S.

We also tested for protein complexes containing both GLD-2 and GLD-3 proteins in worm extracts. To this end, we immunoprecipitated GLD-2 using anti-GLD-2 antiserum bound to protein G beads. Specifically, we incubated extracts prepared from mixed stage worms with beads carrying either anti-GLD-2 antibodies or preimmune serum. GLD-3L antibodies recognized a band of the correct size in the GLD-2 immunoprecipitate, but did not recognize any band in the precipitate using preimmune serum (Figure 3C). We conclude that GLD-2 and GLD-3 are associated with each other in nematodes, consistent with the idea that they work together to control the mitosis/meiosis decision.

Do *gld-2* and *gld-3* promote meiosis in *fbf-1 fbf-2* double mutants? Whereas wild-type germlines make >1000 descendants/gonadal arm, the *fbf-1 fbf-2* double mutant generates only ~70 germ cells/arm, and all of these enter meiosis and make sperm (CRITTENDEN *et al.* 2002; Table 3; Figure 5A). By contrast, *gld-2* and *gld-3* single mutants have a longer than normal mitotic region. To determine if *gld-2* or *gld-3* is required for abnormal entry into meiosis in *fbf-1 fbf-2* double mutants, we examined *gld-2; fbf-1 fbf-2* and *fbf-1 fbf-2 gld-3* triple-mutant germlines. On average, these triple mutants [and the quadruple *gld-2; fbf-1 fbf-2 gld-3(RNAi)*] made about twice as many germ cells as the *fbf-1 fbf-2* double mutant (Table 3). We conclude that the mitosis/meiosis defect typical of *gld-2* and *gld-3* single mutants, which is an increased capacity for mitosis, was also observed in the triple and quadruple mutants that lack both *fbf* and *gld* activities. Therefore, *fbf* appears to act upstream of *gld-2* and *gld-3* (also see below).

In contrast to the effect of *gld-2* and *gld-3*, removal of *nos-3* had a more dramatic effect. Whereas *nos-3* germlines have no detectable effect on the mitosis/meiosis decision (Table 2), *fbf-1 fbf-2 nos-3* germlines made ~500 descendants/gonadal arm (Table 3; HANSEN *et al.* 2004). This effect is more dramatic than that of *gld-2* or *gld-3* and is reminiscent of *gld-1; fbf-1 fbf-2* germlines, which are fully tumorous (CRITTENDEN *et al.* 2002). We conclude that *nos-3* is critical for promoting meiosis in the absence of FBF.

The *nos-3* gene acts in the *gld-1* branch and parallel to *gld-2/gld-3* to promote meiosis: To determine how *nos-3* fits into the regulatory pathway controlling mitosis/meiosis, we examined the transition from mitosis to meiosis in double and triple mutants (Figure 4; Table 4). No

TABLE 3

Effect of *gld* and *nos-3* mutants on *fbf* proliferation defect

Genotype[a]	Average no. of germ cells/arm (range)[b]	*n*
Wild type[c]	>1000	>50
fbf-1 fbf-2[d]	70 (49–107)	18
gld-2; fbf-1 fbf-2	117 (75–235)	19
fbf-1 fbf-2 gld-3	127 (58–229)	25
gld-2; fbf-1 fbf-2 gld-3(RNAi)	119 (58–253)	16
fbf-1 fbf-2 nos-3	509 (395–606)	5

n, number of germlines scored.

[a] All mutations were strong loss-of-function putative nulls (see MATERIALS AND METHODS).

[b] Range indicates lowest and highest germ cell counts in data sets.

[c] Wild type was first reported by KIMBLE and WHITE (1981) and confirmed here. Number is approximate and range was not determined.

[d] *fbf-1 fbf-2* was first reported by CRITTENDEN *et al.* (2002), but repeated here in parallel with the other experiments for comparison.

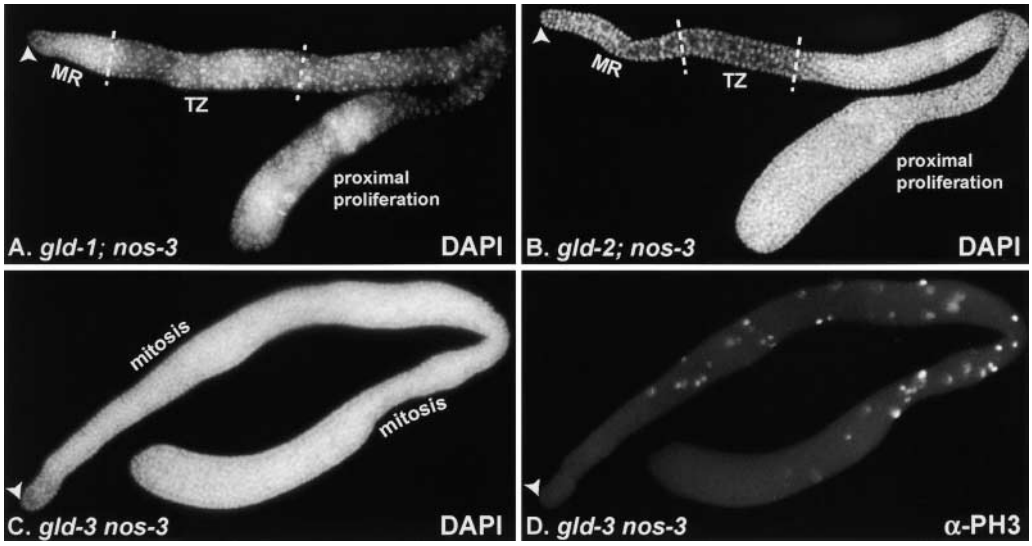

FIGURE 4.—The *gld-3 nos-3* germline is tumorous. Germlines were extruded from adult hermaphrodites at same stage and magnification. (A) *gld-1(q485); nos-3 (q650).* (B) *gld-2(q497); nos-3 (q650).* (C and D) *gld-3 (q730) nos-3(q650).* A–C were stained with DAPI; D was stained with anti-phosphohistone H3. Borders of the transition zone (TZ) are indicated by dashed lines. Arrowhead, distal end of germline.

synergistic effect was seen between the *gld-1* and *nos-3* genes: *gld-1; nos-3* double-mutant germlines were similar to those of *gld-1* single mutants (Figure 4A; Tables 2 and 4; HANSEN *et al.* 2004). By contrast, we did see a synergistic effect between *nos-3* and both *gld-2* and *gld-3*. In *gld-2; nos-3* double mutants, aberrant mitoses were observed in the proximal germline (Figure 4B; HANSEN *et al.* 2004). Such proximal germline mitoses are not typical of either *gld-2* or *nos-3* single mutants, although they are seen in 2% of strong loss-of-function *gld-2(q497)* germlines (KADYK and KIMBLE 1998; KRAEMER *et al.* 1999). More dramatically, *gld-3 nos-3* germlines were uniformly tumorous, as assayed by DAPI staining and antibodies to PH3 (Figure 4, C and D) and antibodies to GLP-1 (not shown). Indeed, we observed no sign of early meiosis in *gld-3 nos-3* germlines. Therefore, both *gld-2* and *gld-3*

TABLE 4

Regulators of entry into meiosis are downstream of *fbf*

Genotype[a]	MR/TZ boundary (range)[b]	TZ/PR boundary (range)[b]	*n*
Wild type	20 (18–21)	30 (28–31)	>50
fbf-1 fbf-2	None[c]	None[c]	18
gld-1 gld-2	Tumorous	Tumorous	22
gld-1 gld-2; fbf-1 fbf-2	Tumorous	Tumorous	9
gld-1; gld-3(RNAi)	Tumorous	Tumorous	60
gld-1; fbf-1 fbf-2 gld-3(RNAi)	Tumorous	Tumorous	52
gld-2; nos-3	20 (17–23)	34 (29–40)	11
gld-2; fbf-1 fbf-2 nos-3	27 (24–34)	45 (37–50)	5
gld-3(q730) nos-3 or *gld-3(RNAi) nos-3*	Tumorous	Tumorous	94
fbf-1 fbf-2 gld-3(q730) nos-3 or *fbf-1 fbf-2 gld-3(RNAi) nos-3*	51 (28–70)	68 (36–103)	20
gld-1; nos-3	15 (12–19)	30 (22–37)	17
gld-1; fbf-1 fbf-2 nos-3	Tumorous	Tumorous	2
gld-2; gld-3(RNAi)	29 (24–34)	52 (41–58)	18
gld-2; fbf-1 fbf-2 gld-3(RNAi)	None[c]	None[c]	25

n, number of germlines scored; MR, mitotic region; TZ, transition zone; PR, pachytene region; see Figure 1 and text for explanation.

[a] All mutations were strong loss-of-function putative nulls (see MATERIALS AND METHODS). Animals were observed 24 hr after mid-L4.

[b] Range indicates the shortest boundary and the longest boundary observed.

[c] All germ cells are in meiosis.

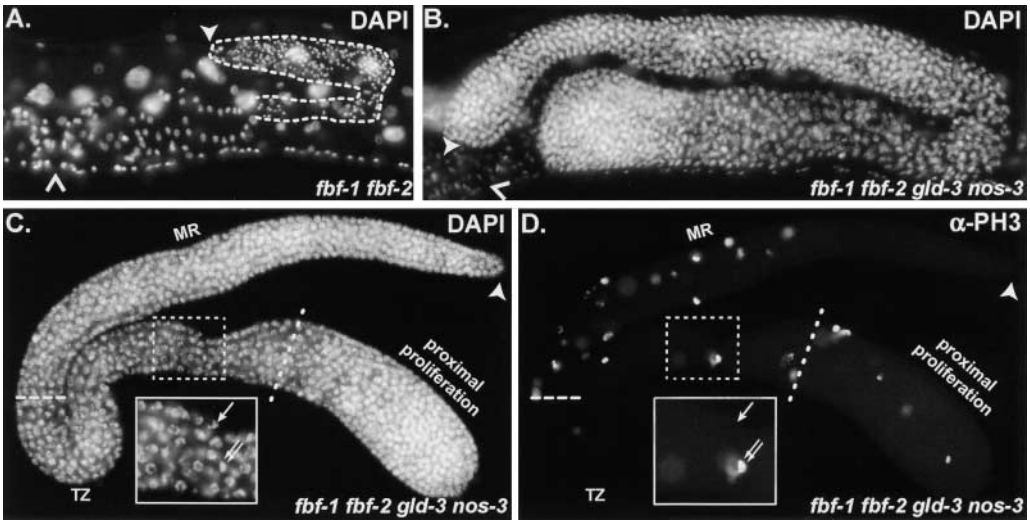

FIGURE 5.—*gld-3 nos-3* germline is tumorous in the absence of *fbf-1 fbf-2*. (A and B) Whole mounts, DAPI stained. Posterior region of adults is at same stage and magnification; caret marks vulva; arrowhead marks distal end of germline. (A) *fbf-1 fbf-2* double mutant. Dashed line demarcates germline. All germ cells have entered meiosis and matured into sperm. (B) *fbf-1 fbf-2 gld-3 nos-3* quadruple mutant. Germline is grossly proliferative. (C and D) Extruded *fbf-1 fbf-2 gld-3 nos-3* germline. C is DAPI stained. (D) Anti-phosphohistone H3 marks mitotic nuclei. The mitotic region expands proximally, and additional proliferation occurs at the proximal end. Borders of the transition zone (TZ) are indicated by dashed lines; TZ is not normal in that mitotic figures and anti-PH3 positive nuclei can be present (see inset). Pachytene nuclei can also be found within the TZ near its proximal border. In insets, small arrow points to meiotic nucleus, and double arrow points to mitotic nucleus that is anti-PH3 positive.

exhibit synergistic defects with *nos-3*, but the effect is more severe with *gld-3*.

The difference between the *gld-2; nos-3* and *gld-3 nos-3* double-mutant germlines underscores the idea that *gld-2* and *gld-3* do not have identical roles in maintaining the mitosis/meiosis decision. Because *nos-3* is not synergistic with *gld-1*, but is synergistic with both *gld-2* and *gld-3*, albeit at different levels, we suggest that *nos-3* acts in the same regulatory branch as *gld-1* to promote meiosis (Figure 9A; see also HANSEN *et al.* 2004). Furthermore, we suggest that *nos-3* acts in parallel with *gld-3* to control entry into meiosis and in parallel with *gld-2* to maintain commitment to meiosis. This difference between the effects of *gld-2* and *gld-3* may reflect the reciprocal repression between FBF and GLD-3 (see DISCUSSION).

Regulatory relationship between *fbf* and *gld/nos* genes: We next investigated epistasis in quadruple mutants, which included the *fbf-1 fbf-2* double mutant in combination with various synthetic tumorous double mutants. All germlines were scored in young adults, when *fbf-1 fbf-2* germlines normally have no mitotic cells, but instead consist solely of mature sperm (Figure 5A). By contrast, the *gld-1 gld-2; fbf-1 fbf-2* and *gld-1; fbf-1 fbf-2 gld-3(RNAi)* germlines were fully tumorous (Table 4). This tumorous state was similar to that of the *gld-1; fbf-1 fbf-2* triple mutant reported previously (CRITTENDEN *et al.* 2002).

The *fbf-1 fbf-2 gld-3 nos-3* and *gld-2; fbf-1 fbf-2 nos-3* quadruple-mutant germlines were also largely tumorous: they proliferated more than any of the triple mutants (*fbf-1 fbf-2 gld-3, gld-2; fbf-1 fbf-2*, or *fbf-1 fbf-2 nos-3*; Figure 5B; not shown). In both quadruple mutants, the distal mitotic region was even longer than that in *gld-2* or *gld-3* single mutants and proximal mitoses were consistently observed (Figure 5, C and D). However, the germlines did enter meiosis. Therefore, the *gld-3 nos-3* tumor is not completely epistatic to *fbf-1 fbf-2*. We suggest that this partial epistasis may reflect reciprocal repression between FBF and GLD-3 (see DISCUSSION), although alternative explanations are plausible.

FBF binds elements in the *gld-3S* 3′-UTR: To ask whether *gld-3* might be a direct target of FBF, we examined the sequence of its 3′-UTRs for potential FBF-binding sites. All known PUF-binding sites contain a core UGU(G/A) tetranucleotide, but FBF does not bind specifically to all such sequences (WICKENS *et al.* 2000). We therefore scanned 3′-UTRs for this core sequence in a context similar to that found for established FBF-binding sites in *fem-3* and *gld-1* mRNAs (ZHANG *et al.* 1997; CRITTENDEN *et al.* 2002). The *gld-3* gene expresses two major transcripts, *gld-3L* and *gld-3S* (Figure 8A). Two potential sites in the *gld-3L* 3′-UTR were tested by three-hybrid assay, but they did not bind FBF-1 (data not shown). However, FBF-1 and FBF-2 did interact specifically with two of the three potential sites identified within the 191-nt 3′-UTR of the *gld-3S* mRNA (Figure 6). By three-hybrid assay, a region covering two closely linked core elements (FBE-a and FBE-b) in the *gld-3S* 3′-UTR (Figure 6A) interacted strongly and reproducibly with FBF (Figure 6, B and C). Furthermore, individual sequence elements FBE-a and FBE-b were sufficient to bind FBF in yeast three-hybrid assays (Figure 6, B and C). Indeed, both of these sites are strongly conserved in *gld-3S* 3′-UTRs from each of the three Caenorhabditis family members (Figure 6A, bottom). Another putative site (FBE-c, Figure 6A) did not bind FBF, although it expressed well in yeast (Figure 6, B and C; data not shown). In gel shifts, a fragment carrying both FBE-a and FBE-b sites was bound *in vitro* by purified FBF protein (Figure 6D, left), as was a fragment carrying only

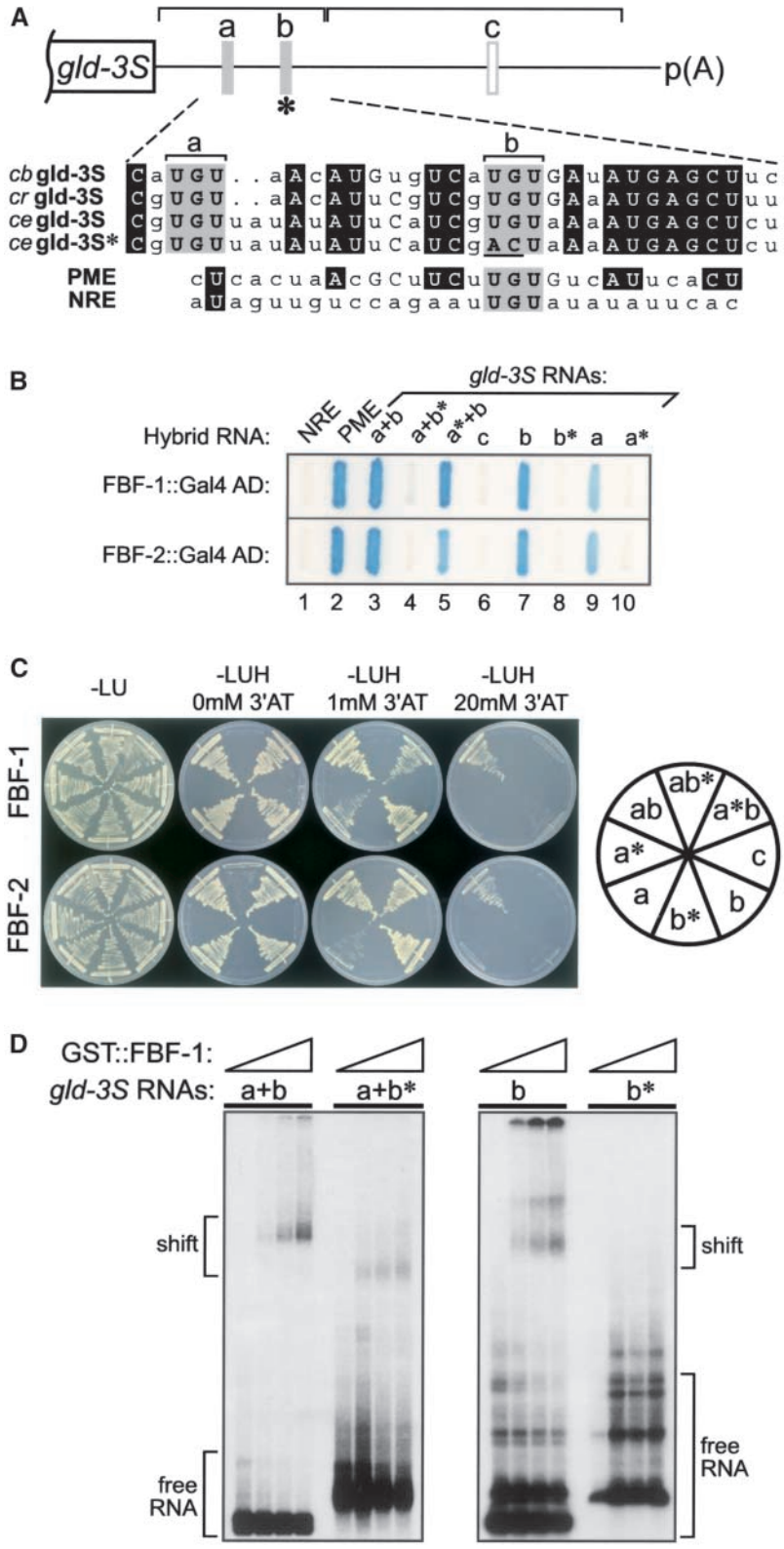

FIGURE 6.—*fbf* binds specifically to *gld-3S* 3′-UTR. (A) Schematic of *gld-3S* 3′-UTR. p(A), poly(A)$^+$ tail; brackets, regions tested for binding; gray boxes, predicted FBF-binding elements (*e.g.*, a, FBE-a); only solid boxes bind FBF (see below). Shown is sequence alignment of FBE-a and FBE-b from three Caenorhabditis species (*cb*, *C. briggsae*; *cr*, *C. remanei*; *ce*, *C. elegans*; solid boxes, identical nucleotides). PME, FBF-binding region in *fem-3* 3′-UTR; NRE, Pumilio-binding region in *hunchback* 3′-UTR. The PME and NRE serve as positive and negative controls for FBF binding, respectively. Underlined nucleotides, artificially engineered mutation in FBE-b (a similar mutation was made in FBE-a); asterisks, mutated elements. (B and C) Yeast three-hybrid analysis of predicted FBF-binding sites. In both B and C, interactions with FBF-1 are shown at the top, and interactions with FBF-2 are shown at the bottom. (B) β-Galactosidase activity. (C) *HIS3* reporter activation. Growth was monitored on media lacking histidine and containing varying concentrations of *HIS3* competitor 3-AT. (D) Gel retardation assays. Radiolabeled RNAs were incubated with 0, 50, 100, 200 pmol GST::FBF-1, from left to right. FBF-1 forms a slower migrating complex specifically with a fragment containing FBE-a and FBE-b (left) or FBE-b alone (right).

the FBE-b site (Figure 6D, right). As controls for specificity, we mutated the first two core nucleotides, which abolished binding for the individual sequence elements FBE-a and FBF-b. We conclude that FBF-1 and FBF-2 bind specifically to two sites within the *gld-3S* 3′-UTR.

FBF controls GLD-3 expression: To further test the idea that FBF represses *gld-3* expression, we compared the level of GLD-3 protein in wild-type and *fbf-1 fbf-2* germlines by immunocytochemistry (Figure 7). Specifically, we examined GLD-3 in late L3 or early L4 males using affinity-purified antibodies that recognize both GLD-3S and GLD-3L (ECKMANN *et al.* 2002). We used

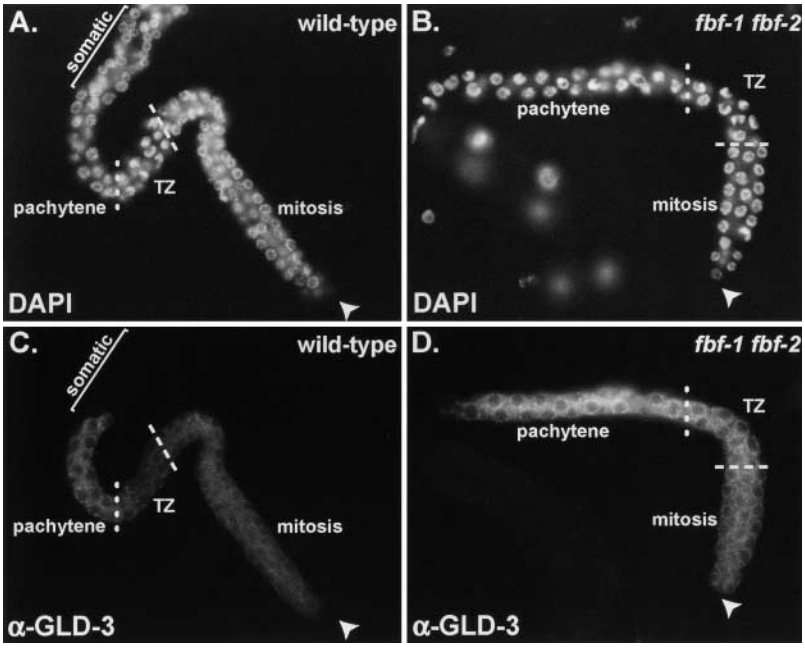

FIGURE 7.—*fbf* represses *gld-3* expression *in vivo*. (A–D) Epifluorescent images of male germlines in late L3 or early L4 of wild type (A and C) and *fbf-1 fbf-2* (B and D) stained with DAPI (A and B) and anti-GLD-3 (C and D). Borders between mitotic region, transition zone (TZ), and pachytene region are indicated by dashed lines. Arrowhead, distal end of germline. (C and D) GLD-3 protein was detected using a polyclonal antibody that recognizes both GLD-3S and GLD-3L; attempts to make a GLD-3S-specific antibody were not successful. The level of GLD-3 protein is reproducibly elevated in *fbf-1 fbf-2* mutants compared to the wild type. This elevation is seen in all germ cells, especially those in the transition zone. Extruded germlines were treated identically and all comparative pictures were taken with the same settings and have the same magnification.

immunocytochemistry rather than Western blots in this experiment because GLD-3 levels vary with position and we wanted to monitor expression at specific locations in the germline (ECKMANN *et al.* 2002; Figure 7, C and D). We used males in this experiment to eliminate sexual differences between the two germlines (both wild-type males and *fbf-1 fbf-2* mutants make sperm only), and we used late L3 or early L4 animals to ensure the presence of mitotic, transition, and pachytene regions (*fbf-1 fbf-2* mutants lose their mitotic region in late L4 or adulthood). Wild-type and mutant germlines were stained in parallel and images were captured and processed using identical settings.

In wild-type males, the midlarval germline has a distal mitotic region, a transition zone, and some pachytene cells (Figure 7A). The same regions are present in *fbf-1 fbf-2* males in larval stage four (Figure 7B). In the wild type, GLD-3 was detectable, but only at a low level in the mitotic region, barely detectable in the transition zone, and higher in the pachytene region (Figure 7C). In contrast, the majority (65%, $n = 20$) of *fbf-1 fbf-2* germlines displayed higher levels of GLD-3 protein than did wild type in all three regions (Figure 7D), but some (25%, $n = 20$) showed higher GLD-3 levels restricted to the TZ and the pachytene region. The remaining 10% ($n = 20$) showed no difference in GLD-3 levels. The anti-GLD-3 antibodies recognize both GLD-3L and GLD-3S, so we cannot exclude the possibility that FBF regulates *gld-3L* expression as well. We conclude that FBF negatively regulates GLD-3 expression and suggest that FBF represses *gld-3* directly by binding an element in the *gld-3S* mRNA.

GLD-3 protein contains two distinct regulatory domains: Using a standard PCR-based method to screen for deletion mutants, we isolated *gld-3(q741)*, which removes most of the C-terminal region from GLD-3, including the FBF-binding domain (ECKMANN *et al.* 2002; Figure 8A). Wild-type animals make two major GLD-3 proteins, GLD-3L and GLD-3S (Figure 8B, lane 1), and the strong loss-of-function *gld-3(q730)* mutant makes no detectable GLD-3 protein (Figure 8B, lane 2; ECKMANN *et al.* 2002). In *gld-3(q741)* homozygotes, we observed two major proteins (Figure 8B, lane 3): the larger protein in lane 3 corresponds in size to *in vitro* translated protein from a *gld-3L(Δ)* cDNA carrying the same deletion as *q741* (Figure 8B, lane 4), and the smaller protein in lane 3 corresponds in size to *in vitro* translated GLD-3S (Figure 8B, lane 5). Therefore, *gld-3(q741)* homozygotes express full-length GLD-3S protein and a stable truncated version of GLD-3L.

We next examined the mitosis/meiosis and sperm/oocyte decisions in *gld-3(q741)* homozygotes. The mitotic region of *gld-3(q741)* germlines was similar to that of wild type, albeit slightly longer (Table 2). Therefore, GLD-3 protein that retains its GLD-2-binding region, but lacks an FBF-binding region, does not have the dramatic mitosis/meiosis delay seen in *gld-3* null mutants. By contrast, sex determination was not normal; *gld-3(q741)* males produced oocytes, as assayed by both Nomarski appearance (Figure 8C) and anti-RME-2 staining (100%, $n = 45$). We suggest that the primary role of GLD-3 protein in the mitosis/meiosis decision is carried out by its interaction with GLD-2 and that its primary role in the sperm/oocyte decision relies on its interaction with FBF. Consistent with this interpretation, the *gld-3(q741) nos-3(q650)* double-mutant germ cells enter meiosis (data not shown).

DISCUSSION

This article focuses on GLD-3 and its control of the mitosis/meiosis decision in the *C. elegans* germline. Our

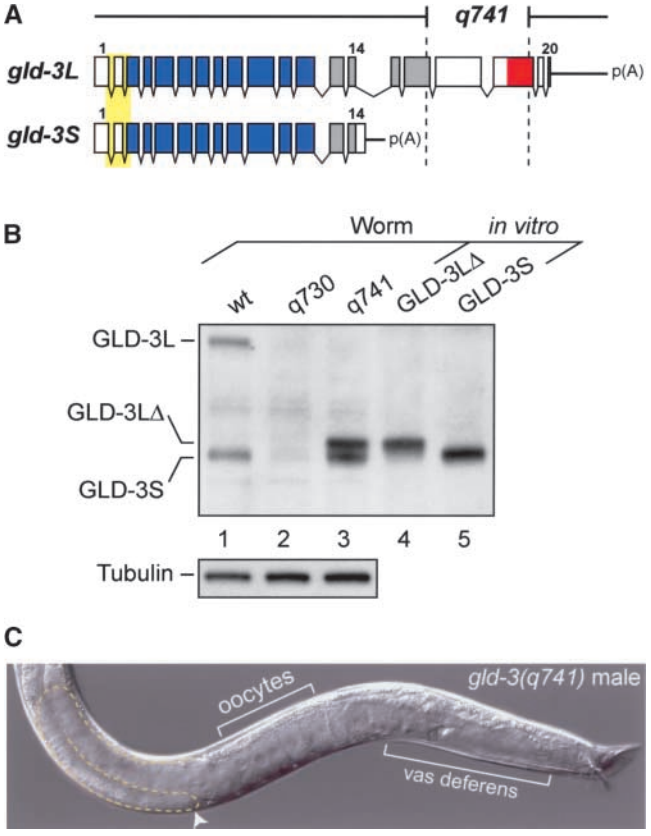

Figure 8.—GLD-3L-specific deletion mutant affects sex-determination but not the mitosis/meiosis decision. (A) Molecular lesion in *gld-3(q741)*. Two *gld-3* transcripts, *gld-3S* and *gld-3L*, are drawn to scale. Boxes, exons; lines, introns. The *gld-3(q741)* deletion (1154 bp, nt 2921–4076) is shown above transcripts. Colors of GLD-3 motifs are as in Figure 3A. Yellow box, GLD-2-binding region in shared GLD-3 N terminus. (B) GLD-3 proteins. Western blots of extracts were prepared from adult hermaphrodites of the following genotypes: lane 1, wild type (wt); lane 2, *gld-3(q730)*; lane 3, *gld-3(q741)*; lane 4, *in vitro* translated GLD-3L(Δ); lane 5, *in vitro* translated GLD-3S. Tubulin was used as a loading control (lower blot). (C) Adult *gld-3(q741)* male. Germline has normal size, but makes oocytes in addition to a few sperm (not visible in this image).

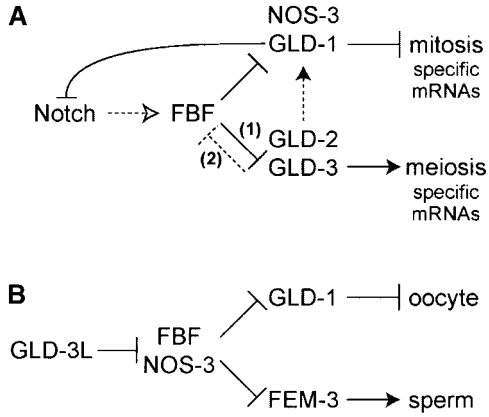

Figure 9.—Regulatory circuits controlling mitosis/meiosis and sperm/oocyte decisions. (A) Regulatory circuit for mitosis/meiosis decision. Two major regulatory branches control entry into meiosis. We propose that GLD-1 and NOS-3 regulators promote entry into meiosis by repressing mRNAs critical for mitosis and that GLD-2 and GLD-3 do so by activating mRNAs critical for meiosis. GLD-1/NOS-3 and GLD-2/GLD-3 branches act largely in parallel. We also propose that FBF promotes continued mitotic divisions by repressing at least one mRNA in each major regulatory branch: *gld-1* and *gld-3S*. In addition, we suggest that reciprocal repression plays a minor role in controlling this decision: (1) FBF repression of *gld-3* expression appears to be the primary regulatory relationship between FBF and *gld-3*, but (2) GLD-3 antagonism of FBF may play a minor role. Notch signaling promotes mitosis, perhaps by activating FBF, either directly or indirectly (dashed arrow). We have also found that *gld-3 nos-3* is epistatic to *glp-1(RNAi)*, consistent with a position of *gld-3* downstream of GLP-1 signaling (data not shown). We further note that FBF affects the GLD-1/NOS-3 branch more dramatically than the GLD-2/GLD-3 branch, and other regulators are likely to be involved. (B) Regulatory circuit for sperm/oocyte decision. FBF promotes oogenesis by repressing *gld-1* and *fem-3*. In addition, NOS-3 promotes oogenesis. GLD-2 plays no known role in the sperm/oocyte decision, but GLD-3L is critical for continued spermatogenesis in males, which it achieves by antagonizing FBF. See text for further explanation and references.

results support four major conclusions. First, GLD-3 works together with GLD-2 to control the mitosis/meiosis decision. Second, GLD-3 acts in parallel to GLD-1 and NOS-3 in the regulatory network controlling mitosis or meiosis. Third, FBF represses *gld-3* expression. And fourth, the molecular mechanisms by which GLD-3 controls the mitosis/meiosis and sperm/oocyte decisions are largely distinct. Our discussion places these results in the context of a regulatory circuit that controls the mitosis/meiosis decision and contrasts that circuit and its molecular underpinnings to one controlling the sperm/oocyte decision (Figure 9). Collectively, our results demonstrate how a molecular switch can be modified and refined to control distinct decisions, *e.g.*, mitosis/meiosis and sperm/oocyte, in a developing tissue.

GLD-3 acts with GLD-2 to promote entry into meiosis: The *gld-2* gene controls entry into meiosis (Kadyk and Kimble 1998), but the role of *gld-3* in this process had not been explored. Instead, *gld-3* was known to function in the sperm/oocyte decision, germline survival, progression through meiosis, and early embryogenesis (Eckmann *et al.* 2002). The discovery that GLD-3 partners with GLD-2 to form a poly(A) polymerase (Wang *et al.* 2002) raised the question of whether GLD-3 might work together with GLD-2 to control entry into meiosis. In this article, we provide several lines of evidence that this is the case. First, both *gld-2* and *gld-3* function in parallel with *gld-1* to direct meiosis (Kadyk and Kimble 1998; this article). Second, both *gld-2* and *gld-3* single mutants fail to enter meiosis at the normal position, but instead both enter meiosis more proximally than normal. And third, the *gld-2; gld-3* double mutant is indistinguishable from either single mutant with respect to entry into meiosis. The idea that GLD-2 and GLD-3 act together as a protein complex is supported by identification of a specific region within GLD-3 that is responsible for binding to GLD-2 as well as by their co-immunoprecipitation from worm extracts. Therefore, both genetic and molecular

lines of evidence support the idea that GLD-2 and GLD-3 act together to control germline fates and, in particular, that they control entry into meiosis.

In addition to their ability to function together, GLD-2 and GLD-3 also have distinct roles in germline development. For example, GLD-3 is required for maintenance of spermatogenesis in male germlines (Eckmann *et al.* 2002), while GLD-2 is apparently not involved in this process (Kadyk and Kimble 1998). Similarly, GLD-3 is required for germline survival (Eckmann *et al.* 2002), while GLD-2 has not been implicated in this process. Finally, most germ cells in *gld-2; gld-3* double mutants arrest in pachytene (this work), whereas those in single mutants progress into diplotene (Kadyk and Kimble 1998; Eckmann *et al.* 2002), suggesting that GLD-2 and GLD-3 act independently to control the transition from pachytene to diplotene. We envision that GLD-2 and GLD-3 interact with distinct proteins to accomplish their individual roles in germline development. For example, GLD-2 may interact with other RNA-binding proteins in addition to GLD-3 to polyadenylate mRNAs that are different from those targeted by the GLD-2/GLD-3 heterodimer. And GLD-3 may interact with other proteins to accomplish its unique roles. Consistent with this idea, GLD-3 promotes continued spermatogenesis by antagonizing FBF (Eckmann *et al.* 2002).

Two regulatory branches promote entry into the meiotic cell cycle: Entry into meiosis is controlled by two major regulatory branches (Kadyk and Kimble 1998; Hansen *et al.* 2004; this work; Figure 9A). The GLD-1 and NOS-3 proteins reside in one branch, and GLD-2 and GLD-3 reside in the other. The GLD-1/NOS-3 branch is defined by two translational repressors (Jan *et al.* 1999; Kraemer *et al.* 1999; Lee and Schedl 2001; Marin and Evans 2003; Ryder *et al.* 2004). One simple model is that the GLD-1/NOS-3 branch represses mRNAs that promote mitosis (Figure 9A). Of particular note in this context, GLD-1 represses *glp-1* mRNA (Marin and Evans 2003), which encodes the GLP-1/Notch receptor essential for germline mitoses (Crittenden *et al.* 2003). Therefore, GLD-1 ensures entry into meiosis, at least in part, by acting in a negative feedback loop to inhibit a mitosis-promoting regulator.

The GLD-2/GLD-3 regulatory branch is defined by two subunits of an atypical poly(A) polymerase (Wang *et al.* 2002). We suggest that GLD-2 and GLD-3 may polyadenylate and activate meiosis-promoting mRNAs (Figure 9A); in other systems, polyadenylation usually stimulates mRNA expression (Groisman *et al.* 2002). One possible target of the GLD-2/GLD-3 poly(A) polymerase is *gld-1* mRNA; preliminary results indicate that the *gld-1* poly(A) tail is shorter in *gld-2* mutants than in wild type (N. Suh and J. Kimble, unpublished observations). In addition, Hansen *et al.* (2004) found that *gld-2* and *nos-3* act redundantly to control GLD-1 protein accumulation, which led them to suggest that *gld-1* might be a GLD-2 target (Hansen *et al.* 2004). Although *gld-1* mRNA may indeed be one direct target, GLD-2/GLD-3 poly(A) polymerase must target additional mRNAs since GLD-2 can promote meiosis in the absence of GLD-1 activity.

The GLD-1/NOS-3 and GLD-2/GLD-3 regulatory branches are redundant for entry into meiosis, but they most likely exert their effects by opposite molecular mechanisms—RNA repression for GLD-1/NOS-3 and activation for GLD-2/GLD-3. Such a dual mechanism drives the switch from mitosis to meiosis by simultaneously turning on meiosis-specific activities and turning off mitosis-specific activities. That dual mechanism also makes the circuit remarkably robust, a feature that would be selected to control fundamental decisions central to the survival of the species.

A similar two-pronged mechanism controls mating type in the yeast *Saccharomyces cerevisiae*, but does so at the level of transcription. In this case, the *MAT*α mating-type allele encodes α1, a positive regulator of α-specific gene transcription as well as α2, a negative regulator of **a**-specific gene transcription; as a result, yeast cells carrying *MAT*α adopt an α-specific fate, turning on α-specific genes and turning off **a**-specific genes (Herskowitz 1989). The same basic logic regulates entry into meiosis in *C. elegans*, but here the circuitry relies on RNA controls instead of DNA controls.

FBF inhibits both major meiosis-promoting branches: FBF promotes mitosis by repressing mRNAs in both of the major meiosis-promoting regulatory branches (Figure 9A). Specifically, it represses both *gld-1* expression (Crittenden *et al.* 2002) and *gld-3* expression (this work). Thus, FBF binds specifically to sites within the *gld-1* and *gld-3S* 3′-UTRs, and the abundance of GLD-1 and GLD-3 proteins is increased in *fbf* mutants. Mutant analysis is consistent with the idea that FBF represses *gld-3*: when *gld-3* is removed from an *fbf-1 fbf-2* double mutant, an extra cell division occurs. However, a complexity in the interpretation of these results arises from a comparison of the *gld-3 nos-3* and *fbf-1 fbf-2 gld-3 nos-3* germline tumors. Although both strains display vastly overproliferating germlines, the former is fully tumorous, while the latter possesses some cells that have entered meiosis. Therefore, loss of *fbf* does have a minor effect on the *gld-3 nos-3* tumorous phenotype. This lack of complete epistasis may be explained by reciprocal repression between FBF and GLD-3 (Figure 9A; see below), although other explanations are possible.

FBF/GLD balance controls size of the mitotic region: A balance between FBF and GLD-2/GLD-3 activities appears to control the number of cells committed to mitosis or meiosis. *fbf-1* single mutants possess a smaller mitotic region than normal, suggesting that a full complement of both FBF-1 and FBF-2 activities is required to achieve a normally sized mitotic region (Crittenden *et al.* 2002). By contrast, *gld-2* and *gld-3* mutants have a larger mitotic region than normal (this work). Therefore, GLD-2 and GLD-3 are also required for a normally

sized mitotic region, but their effect is opposite to that of FBF. In the case of GLD-1, the mitotic region becomes smaller, which we do not yet understand, but Hansen *et al.* (2004) suggest that GLD-1 affects the size of the mitotic region. Taking these results together, we suggest that a balance between FBF and GLD-2/GLD-3 controls cell number in the mitotic region. In an *fbf-1* mutant, which has less FBF than normal, the balance is tipped toward GLD activity and premature meiosis; in *gld-2* and *gld-3* mutants, the balance is tipped in favor of FBF and extended mitosis.

Distinct roles of GLD-3 in the mitosis/meiosis and sperm/oocyte decisions: GLD-3 has distinct roles in the mitosis/meiosis and sperm/oocyte decisions (Figure 9, A and B). In the sperm/oocyte decision, *gld-3* acts upstream of *fbf* (Eckmann *et al.* 2002), but in the mitosis/meiosis decision, *gld-3* acts largely downstream of *fbf* (this work). At a molecular level, GLD-3L protein can bind FBF and antagonize FBF RNA-binding activity (Eckmann *et al.* 2002) and, conversely, FBF can bind the *gld-3S* 3′-UTR and repress *gld-3* expression (this work). Therefore, the *fbf* and *gld-3* genes are capable of reciprocal repression.

We find that the two opposing FBF/GLD-3 regulatory mechanisms are differentially important for the mitosis/meiosis and sperm/oocyte decisions. Essential to this argument is *gld-3(q741)*, a deletion mutant that removes the FBF-binding region from GLD-3L, but leaves its GLD-2-binding region and KH motifs intact. The germlines of *gld-3(q741)* homozygotes enter meiosis at a position close to that of the wild type, but fail to make sperm continuously in males. Therefore, the FBF-binding region of GLD-3 is crucial for the sperm/oocyte decision, but it plays a minor role, if any, in the mitosis/meiosis decision. The presence of distinct regulatory domains raises the possibility that GLD-3 was co-opted into control of sex determination by incorporation of an FBF-binding region into one of its isoforms.

The mitosis/meiosis and sperm/oocyte regulatory circuits and their evolution: Many mitosis/meiosis regulators also control the sperm/oocyte decision (Table 1). And both circuits control cell number: *fbf-1* mutants have fewer mitotic cells and more sperm, while *gld-3* mutants have more mitotic cells and fewer sperm (Crittenden *et al.* 2002; Eckmann *et al.* 2002; this work). Nonetheless, only one regulatory relationship is fully conserved in the two circuits. FBF represses *gld-1* mRNA in both circuits, but all the other regulators appear to have different roles (Figure 9, A and B). GLD-2 is a key regulator of meiosis, but has no known role in sex determination (Kadyk and Kimble 1998); GLD-3 works downstream of FBF to promote meiosis, but acts primarily upstream of FBF in sex determination (Eckmann *et al.* 2002; this work); and NOS-3 promotes meiosis in the GLD-1 regulatory branch (Hansen *et al.* 2004; this work), but works with FBF to promote oogenesis (Kraemer *et al.* 1999). Therefore, although composed of largely the same regulators, the two pathways have diverged considerably. The mechanism by which two distinct pathways operate in the same tissue to control two distinct sets of fates is not known, but it is likely to involve separation of the regulators in time or space.

We suggest that the mitosis/meiosis and sperm/oocyte circuits evolved from an ancient pathway designed to control opposing fates (*e.g.*, mitosis *vs.* meiosis or sperm *vs.* oocyte). The circuit controlling the mitosis/meiosis decision in the *C. elegans* germline can be thought of more broadly as a circuit that controls the balance between growth and differentiation. Analogous circuits are likely to exist in other stem cell systems. Indeed, homologous circuits may control stem cells in other tissues, given the conserved role of PUF proteins in controlling stem cells in *C. elegans* and Drosophila (Lin and Spradling 1997; Forbes and Lehmann 1998; Crittenden *et al.* 2002). In *C. elegans*, we suggest that the mitosis/meiosis and sperm/oocyte circuits have evolved together since they both control early decisions in germline development that must be integrated to achieve the mature tissue. The future challenge is to understand how these overlapping pathways work in both sexes to maintain a stem cell population and yet generate germlines with different gametes.

We thank Tim Schedl for anti-GLD-1, Monique Zetka for anti-HIM-3, Sam Ward for the sperm-specific antibody SP56, Barth Grant for anti-RME-2, and the *Caenorhabditis* Genetics Center (CGC) for providing strains. We thank Dave Hansen, Tim Schedl, and members of the Kimble laboratory for helpful discussions and Beth Thompson, Liana Lamont, Jen Bachorik, Dave Rudel, and the reviewers for comments on the manuscript. We are also grateful to Peggy Kroll-Conner for assistance with generating the *gld-3* deletion mutant and some double and triple mutants on chromosome II and Anne Helsley-Marchbanks and Laura Vanderploeg for help with preparing the manuscript and figures. C.R.E. was supported by a Human Frontiers Science Program Long-Term Fellowship. J.K. is an investigator with the Howard Hughes Medical Institute (HHMI).

LITERATURE CITED

Bernstein, D. S., N. Buter, C. Stumpf and M. Wickens, 2002 Analyzing mRNA-protein complexes using a yeast three-hybrid system: methods and applications. Methods **26:** 123–141.

Brenner, S., 1974 The genetics of *Caenorhabditis elegans*. Genetics **77:** 71–94.

Crittenden, S. L., E. R. Troemel, T. C. Evans and J. Kimble, 1994 GLP-1 is localized to the mitotic region of the *C. elegans* germ line. Development **120:** 2901–2911.

Crittenden, S. L., D. S. Bernstein, J. L. Bachorik, B. E. Thompson, M. Gallegos *et al.*, 2002 A conserved RNA-binding protein controls germline stem cells in *Caenorhabditis elegans*. Nature **417:** 660–663.

Crittenden, S. L., C. R. Eckmann, L. Wang, D. S. Bernstein, M. Wickens *et al.*, 2003 Regulation of the mitosis/meiosis decision in the *Caenorhabditis elegans* germline. Philos. Trans. R. Soc. Lond. B **358:** 1359–1362.

Dernburg, A. F., K. McDonald, G. Moulder, R. Barstead, M. Dresser *et al.*, 1998 Meiotic recombination in *C. elegans* initiates by a conserved mechanism and is dispensable for homologous chromosome synapsis. Cell **94:** 387–398.

Eckmann, C. R., B. Kraemer, M. Wickens and J. Kimble, 2002 GLD-3, a Bicaudal-C homolog that inhibits FBF to control germline sex determination in *C. elegans*. Dev. Cell **3:** 697–710.

Forbes, A., and R. Lehmann, 1998 Nanos and Pumilio have critical roles in the development and function of *Drosophila* germline stem cells. Development **125:** 679–690.

Fox, M. S., and R. A. Reijo Pera, 2001 Male infertility, genetic analysis of the *DAZ* genes on the human Y chromosome and genetic analysis of DNA repair. Mol. Cell. Endocrinol. **184:** 41–49.

Groisman, I., M. Y. Jung, M. Sarkissian, Q. Cao and J. D. Richter, 2002 Translational control of the embryonic cell cycle. Cell **109:** 473–483.

Hansen, D., L. Wilson-Berry, T. Dang and T. Schedl, 2004 Control of the proliferation versus meiotic development decision in the *C. elegans* germline through regulation of GLD-1 protein accumulation. Development **131:** 93–104.

Hendzel, M. J., Y. Wei, M. A. Mancini, A. Van Hooser, T. Ranalli *et al.*, 1997 Mitosis-specific phosphorylation of histone H3 initiates primarily within pericentromeric heterochromatin during G2 and spreads in an ordered fashion coincident with mitotic chromosome condensation. Chromosoma **106:** 348–360.

Herskowitz, I., 1989 A regulatory hierarchy for cell specialization in yeast. Nature **342:** 749–757.

Hubbard, E. J. A., and D. Greenstein, 2000 The *Caenorhabditis elegans* gonad: a test tube for cell and developmental biology. Dev. Dyn. **218:** 2–22.

Jan, E., C. K. Motzny, L. E. Graves and E. B. Goodwin, 1999 The STAR protein, GLD-1, is a translational regulator of sexual identity in *Caenorhabditis elegans*. EMBO J.**18:** 258–269.

Jaruzelska, J., M. Kotecki, K. Kusz, A. Spik, M. Firpo *et al.*, 2003 Conservation of a Pumilio-Nanos complex from *Drosophila* germ plasm to human germ cells. Dev. Genes Evol. **213:** 120–126.

Jones, A. R., and T. Schedl, 1995 Mutations in *gld-1*, a female germ cell-specific tumor suppressor gene in *Caenorhabditis elegans*, affect a conserved domain also found in Src-associated protein Sam68. Genes Dev. **9:** 1491–1504.

Kadyk, L. C., and J. Kimble, 1998 Genetic regulation of entry into meiosis in *Caenorhabditis elegans*. Development **125:** 1803–1813.

Kamath, R. S., and J. Ahringer, 2003 Genome-wide RNAi screening in *Caenorhabditis elegans*. Methods **30:** 313–321.

Kimble, J. E., and J. G. White, 1981 On the control of germ cell development in *Caenorhabditis elegans*. Dev. Biol. **81:** 208–219.

Kraemer, B., S. Crittenden, M. Gallegos, G. Moulder, R. Barstead *et al.*, 1999 NANOS-3 and FBF proteins physically interact to control the sperm-oocyte switch in *Caenorhabditis elegans*. Curr. Biol. **9:** 1009–1018.

Lee, M.-H., and T. Schedl, 2001 Identification of in vivo mRNA targets of GLD-1, a maxi-KH motif containing protein required for *C. elegans* germ cell development. Genes Dev. **15:** 2408–2420.

Lin, H., and A. C. Spradling, 1997 A novel group of *pumilio* mutations affects the asymmetric division of germline stem cells in the *Drosophila* ovary. Development **124:** 2463–2476.

Marin, V. A., and T. C. Evans, 2003 Translational repression of a *C. elegans* Notch mRNA by the STAR/KH domain protein GLD-1. Development **130:** 2623–2632.

Martin, G., P. Jeno and W. Keller, 1999 Mapping of ATP binding regions in poly(A) polymerases by photoaffinity labeling and by mutational analysis identifies a domain conserved in many nucleotidyltransferases. Protein Sci. **8:** 2380–2391.

Meng, X., M. Lindahl, M. E. Hyvonen, M. Parvinen, D. G. de Rooij *et al.*, 2000 Regulation of cell fate decision of undifferentiated spermatogonia by GDNF. Science **287:** 1489–1493.

Moore, F. L., J. Jaruzelska, M. S. Fox, J. Urano, M. T. Firpo *et al.*, 2003 Human Pumilio-2 is expressed in embryonic stem cells and germ cells and interacts with DAZ (Deleted in AZoospermia) and DAZ-like proteins. Proc. Natl. Acad. Sci. USA **100:** 538–543.

Ohno, M., A. Segref, A. Bachi, M. Wilm and I. W. Mattaj, 2000 PHAX, a mediator of U snRNA nuclear export whose activity is regulated by phosphorylation. Cell **101:** 187–198.

Raabe, T., K. G. Murthy and J. L. Manley, 1994 Poly(A) polymerase contains multiple functional domains. Mol. Cell. Biol. **14:** 2946–2957.

Ryder, S. P., L. A. Frater, D. L. Abramovitz, E. B. Goodwin and J. R. Williamson, 2004 RNA target specificity of the STAR/GSG domain post-transcriptional regulatory protein GLD-1. Nat. Struct. Mol. Biol. **11:** 20–28.

Spradling, A., D. Drummond-Barbosa and T. Kai, 2001 Stem cells find their niche. Nature **414:** 98–104.

Talerman, A., 1985 Germ cell tumours. Ann. Pathol **5:** 145–157.

Ulbright, T. M., 2004 Gonadal teratomas: a review and speculation. Adv. Anat. Pathol. **11:** 10–23.

Wang, L., C. R. Eckmann, L. C. Kadyk, M. Wickens and J. Kimble, 2002 A regulatory cytoplasmic poly(A) polymerase in *Caenorhabditis elegans*. Nature **419:** 312–316.

Watt, F. M., and B. L. Hogan, 2000 Out of Eden: stem cells and their niches. Science **287:** 1427–1430.

Wickens, M., E. B. Goodwin, J. Kimble, S. Strickland and M. W. Hentze, 2000 Translational control in developmental decisions, pp. 295–370 in *Translational Control of Gene Expression*, edited by N. Sonenberg, J. W. B. Hershey and M. B. Mathews. Cold Spring Harbor Laboratory Press, Cold Spring Harbor, NY.

Wickens, M., D. S. Bernstein, S. L. Crittenden, C. Luitjens and J. Kimble, 2001 PUF proteins and 3′UTR regulation in the *Caenorhabditis elegans* germline. Cold Spring Harbor Symp. Quant. Biol. **66:** 337–343.

Xie, T., and A. C. Spradling, 2000 A niche maintaining germ line stem cells in the *Drosophila* ovary. Science **290:** 328–330.

Yamashita, Y. M., D. L. Jones and M. T. Fuller, 2003 Orientation of asymmetric stem cell division by the APC tumor suppressor and centrosome. Science **301:** 1547–1550.

Zetka, M. C., I. Kawasaki, S. Strome and F. Müller, 1999 Synapsis and chiasma formation in *Caenorhabditis elegans* require HIM-3, a meiotic chromosome core component that functions in chromosome segregation. Genes Dev. **13:** 2258–2270.

Zhang, B., M. Gallegos, A. Puoti, E. Durkin, S. Fields *et al.*, 1997 A conserved RNA-binding protein that regulates sexual fates in the *C. elegans* hermaphrodite germ line. Nature **390:** 477–484.

Communicating editor: A. P. Mitchell